Short review on thermal conductivity of Silicon Nitride Ceramics

Aleksandra B. Šaponjić [1], Slađana LJ. Maslovara [2], Milan V. Gordić [1]

[1] University of Belgrade, „Vinča" Institute of Nuclear Sciences National Institute of the Republic of Serbia, Belgrade, Serbia

[2] Institute of General and Physical Chemistry, Studentski trg 12/V, Belgrade, Serbia

Abstract

One of the most promising substrate materials for the next-generation power devices with high thermal conductivity is silicon nitride (Si_3N_4). There are several ways to improve thermal conductivity of Si_3N_4. Substantially higher thermal conductivities for the Si_3N_4 ceramics could be attained by reduction of lattice oxygen content or by the increasing the β/α phase ratio during nitridation thus enhancing grain growth during post-sintering. The method of purification of the grains and decreasing the two-grain junction films by adding large β-Si_3N_4 grains to the raw Si_3N_4 powder, seeding by grain growth of Si_3N_4 crystals in polycrystalline ceramics also improves thermal conductivity. High thermal conductivity can be further achieved by development a textured microstructure in which elongated β-Si_3N_4 grains are oriented almost unidirectionally. This paper summarizes the extrinsic factors governing the thermal conductivity of Si_3N_4 ceramic regarding microstructural parameters such as lattice defects in single-crystal, sintering additives, change in microstructural parameters like α/β ratio, grain size, aspect ratio, grain orientation and the morphology, composition of grain-boundary, secondary phases, processing method.

Keywords Silicon nitride ceramics; High thermal conductivity; lattice oxygen content, enhancing grain growth, Preparation technique

1. Introduction

Silicon nitride (Si_3N_4) has been studied intensively for more than 60 years and exists in four structural phases: an amorphous a-Si_3N_4, and three crystalline phases, trigonal α-Si_3N_4, hexagonal β-Si_3N_4, and a high-pressure cubic γ-Si_3N_4 phase (or c-Si_3N_4). These crystalline phases are characterized by production routes, compositions, microstructures and underlying all the forms are the fundamental physical and chemical properties of the basic structure each for itself. On heating, a-Si_3N_4 is converted to crystalline α-Si_3N_4; the time–temperature domain boundary for complete crystallization runs from about 10 min at 1400 °C to 1 h at 1250 °C, and to 4 h at 1100 °C. Silicon nitride-based ceramics are polycrystalline materials that consist at least of two phases, the silicon nitride grains and the grain boundary. In general, it is accepted that α-Si_3N_4 is the low-temperature (metastable) modification, and β-Si_3N_4 the stable high-temperature modification at normal pressure [1,2]. The synthesis of γ-Si_3N_4 phase with a cubic spinel structure (see Figure 2.1c) was carried out under high pressure (15 GPa) and at temperatures above 1920 °C in a laser-heated diamond cell [2,3]. Recently, a new δ-Si_3N_4 phase formed in the $Si_{3.0}B_{1.1}C_{5.3}N_{3.0}$ ceramics during annealing at 1800 °C for 3 h under a nitrogen pressure of 10MPa [2].

The recorded terrestrial history of Si_3N_4 spans just longer than 100 years. According to Lord Rayleigh's estimates it is assumed that in the earth's prehistory, when the atmosphere was chemically reducing and rich in ammonia, the crust contained large quantities of silicon and other nitrides [4]. In Nature, Si_3N_4 was found as a mineral, nierite in the perchloric acid resistant residues of primitive meteorites (ordinary chondrites [5] and enstatite chondrites [2,6–8]. This mineral was seen to occur in size 2 μm-0.4 μm, in lathe-shaped grains.

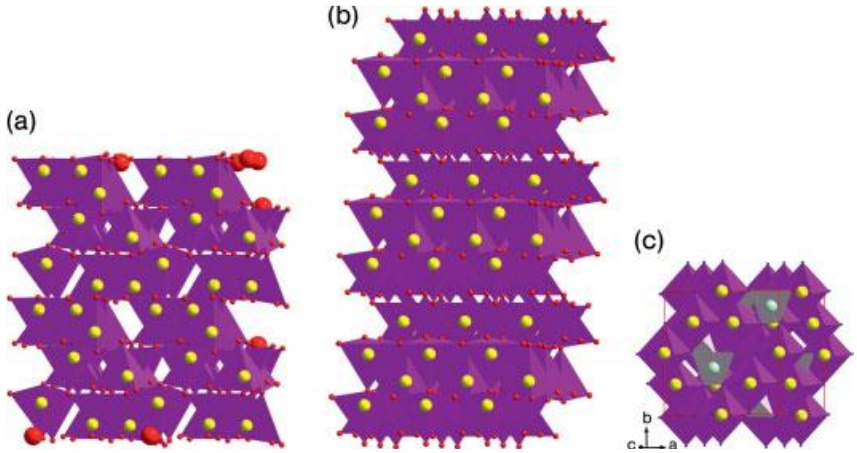

Figure 1. Crystal structures of: (a) α-Si_3N_4; (b) β-Si_3N_4; and (c) γ-Si_3N_4 [2]**.**

Due to excellent electrical and thermal properties, high plasma resistance and chemical stability, high-thermal conductivity which are required in electronic devices, silicon nitride is nowdays is used as dielectric materials in order to dissipate the heat generated from the semiconductor. Also is widely used as packages and substrates for IC products (e.g., accelerometers, gyroscopes, pressure sensors, probe cards, large-scale integration devices, radiofrequency modules, wireless communication devices, light-emitting diodes), optoelectronic products, semiconductor power devices, and so forth [2].

Silicon nitride ceramic (Si_3N_4) is well-known as a high temperature structural ceramic, having high strength and high fracture toughness. Extreme hardness and toughness originate from predominantly covalent bonding and inimitable microstructure, composed of hexagonal, rod-like grains, bonded together reinforcing thus each other [4]. A much attention has been gained to Si_3N_4 as a high-thermal conductivity material, with many research groups having predicted that β-Si_3N_4 crystal would have a high intrinsic thermal conductivity [2].

Due to low self diffusion coefficients nonoxide ceramics with high covalent bonding, such as Si_3N_4, AlN, and SiC even at high temperatures, are densified with the small amounts of sintering additives for development of anisotropic grains actting as reinforcements [9,10]. Low stablillity of Si_3N_4 at higher temperatures is overcome by densification in liquid phase in order to lower the sintering temperatures. Alkaline earth oxides and rare-earth oxides, are used as sintering additives for Si_3N_4 in a wide variety. These additives, during liquid sintering react with impurity oxides largely present as a surface film on the mostly α-Si_3N_4 nitride powder. Densification in Si_3N_4 to form a liquid phase is enhanced through the rearrangement of particles via solution re-precipitation reaction. During liquid-phase sintering α-to-β phase transformation promotes the development of elongated β-Si_3N_4 grains, since α-Si_3N_4 powder is generally used as a starting raw powder [9,11]. Secondary phases thus are formed after sintering, from the liquid phase remaining in the corners of or along the matrix grains as a thin film in a form of glassy or crystalline phases. Typically, the volume fractions of these phases are 5–10%.

2. Factors influencing thermal conductivity of silicon nitride ceramics

2.1. Effect of Impurity Atoms on Thermal Conductivity

The conduction of heat in dielectric ceramics like Si_3N_4 is governed by phonon transport: at room temperature, phonon scattering is substantially affect by imperfections in the crystal lattice, for example, impurity atoms, interstitials, and vacancies. The effect of impurities on thermal conductivities of nonmetallic crystals, was systematically investigated by Slack et al. and revealed the strong correlation between the concentration of lattice oxygen and the thermal conductivity of single crystal [9,12,13]. Heat transfer in silicon nitride that is insulator occurs due to lattice vibration (phonon). Lattice defects in β-Si_3N_4 crystals induce phonon scattering and reduce the thermal conductivity. Therefore, it is essentially important to remove these defects for increasing the thermal conductivity. It has been reported that solution of oxygen into Si3N4 crystals generates defects (vacancies) at sites of Si in crystal lattice .

The two main reasons for sintered silicon nitrides to have lower thermal conductivities are: (i) the distribution of low-thermal conductivity secondary phases resulting from the addition of sintering additives; and (ii) the existence of compositional and crystallographic defects in the grains.

High thermal conductive Si_3N_4 materials [14–18] should fullfield three following conditions: (1) full densification of ceramics must be obtained; (2) lattice oxygen content and lattice defects should be reduced in β- Si_3N_4 grains, since oxygen atoms located in Si_3N_4 lattice generate Si vacancies thus leading to phonon scattering reducing the performance of thermal conduction [9]. This process is explained with the following formula: $2SiO_2 \rightarrow Si_{Si} + 4O_N + V_{Si}$, where O_N and V_{Si} is a dissolved oxygen atom in a nitrogen site and a vacancy in the Si site, respectively. A silicon vacancy is generated in order to maintain electrical neutrality, along with the substitution of O with N. Nitrogen vacancy was confirmed indirectly by measuring the concentration using electron spin resonance (ESR) analyses [19,2].; (3) reduced content of phases in grain boundary should also be provided. Amorphous grain boundary phases between β-Si_3N_4 grains, have very low thermal conductivity value (about 10–15 Wm^{-1} K^{-1}) and large amount of phonon scattering is introduced at the grain boundaries when the lattice vibration encounters, thus reducing the thermal conductivity performance of β-Si_3N_4 ceramics [20].

Silicon nitride after phase transformation, is composed of rodlike grains, reflecting the preferential growth in the [001] direction in β-Si_3N_4 [4]. Crack-bridging processes and toughening of the Si_3N_4 is promoted with these rodlike grains acting as reinforcements. Microstructural factors also affect thermal conductivity in Si_3N_4 (figure 2). Lattice defects in β-Si_3N_4 grains and grain boundary phases originating from sintering additives are considered to be extrinsic factors affecting the thermal conductivity of Si_3N_4 [9].

2.2. Effect of Secondary Phases on Thermal Conductivity

In order to obtained dense Si_3N_4 ceramics with high thermal conductivity liquid-phase sintering with oxides being used as sintering additives as these react with silica impurities located mainly on the Si_3N_4 particle surfaces as an oxidized layer. In this way a liquid phase is formed [4]. A larger amount of sintering additive is required for Si_3N_4 as highly covalent compound (70% covalence) [2,21], due to low stablillity under atmospheric nitrogen pressure at about 2100 K. Exception can be made when sintering via hot-pressing (HP) or hot isostatic pressing (HIP). To decrease the eutectic temperatures with increasing volume fraction of the liquid phase, oxide sintering additives among alkaline-earth oxides, rare-earth oxides, alumina, zirconia, hafnia, and so on are introduced. Though, effective as sintering additive for densification of Si_3N_4, alumina substantial decrease thermal conductivity which is shown experimentally, due to the formation of a solid solution. Substitution Si for Al and N for O leads to formation of β-SiAlON since it dissolves into β-Si_3N_4 lattice. As a consequence, distortion of the lattice cause the difference between the mass of a normal site and a substituted site leading to reduced the thermal conductivity by [9,22,23]. Due to formation of a solid solution (i.e., β-SiAlON) a variety of lattice defects for β-Si_3N_4 grains in sintered Si_3N_4 specimens might be introduced like dissolution of oxygen in β-Si_3N_4 crystals [24,25], dislocations [26], stacking faults [27], and precipitates inside β-Si_3N_4 crystals [28].

Fully dense Si_3N_4 doped with 6 mol% Y_2O_3 or 6 mol% Al_2O_3 with capsule-HIP sintering by Watari et al. and obtained the thermal conductivities of 70 $Wm^{-1}K^{-1}$ and 20 $Wm^{-1}K^{-1}$ [29]. Thermal conductivity with temperature was studied systematically for Si_3N_4 with the variation in content of Y_2O_3, TiO_2, MgO, or Al_2O_3 as additive [16,30–34]. Typically suppression of the thermal conduction indicated in material by point defects for of Si_3N_4 doped with Al_2O_3 had a near-constant value of approximately 20 $Wm^{-1}K^{-1}$ between 300 and 1000 K [35]. In the case of gas-pressure- sintered Si_3N_4 Y_2O_3–Nd_2O_3 exhibited a higher thermal conductivity of over 120 $Wm^{-1}K^{-1}$ related to Si_3N_4 doped with Y_2O_3–Al_2O_3 with thermal conductivity less than 80 $Wm^{-1}K^{-1}$ as reported by Hirosaki [22,27]. Thermal conductivity of Si_3N_4 doped with Y_2O_3–Nd_2O_3 was improved by addition of MgO, but was drastically decreased with the further addition of Al_2O_3 as reported by Okamoto et al. [27,30]. Choice of an adequate sintering additive, excluding alumina can lead to successfully fabricated Si_3N_4 ceramics with a higher thermal conductivity (>100 $Wm^{-1}K^{-1}$). The additive systems chosen by this way are Y_2O_3–Nd_2O_3 [22], Y_2O_3–Nd_2O_3–MgO [30], Y_2O_3–HfO_2 [17], Yb_2O_3–ZrO_2 [36], Yb_2O_3–MgO [37], and so forth. Duan et al. [33] fabricated the Si3N4 ceramics by pressureless sintering with ternary sintering additives. Sample Y_2O_3-MgO- TiO_2 with the mass ratio 2:3:4 showed the highest thermal conductivity of 71 W/(m•K) after sintering and annealing at 1810°C/2 h. With the increasing of dwelling time to 4 hours, the thermal conductivity increases slightly to 74 W/(m•K). the thermal conductivity of gas-pressure sintered Si3N4 sample (1850°C for 3 hours)

So, thermal conductivity of the specimen increases as the ionic radius of the rare-earth element decreases, grain growth of β-Si_3N_4 is enhanced, lattice oxygen of β-Si_3N_4 grains decreases as presented in table 1 [37].

Table 1. Ionic radii of rare earth element, densities, grain sizes, thermal diffusivities, and thermal conductivities of para and perp specimens, and lattice oxygen contents for all samples sintered with different rare earth oxide additives [38]. Para refers to sample of pressed surface of hot-pressed sintered sample; Perp refers to non-pressure surface sample of hot-pressed sintered sample.

Additive	Ionic radius/ nm	Annealing time/h	Density/(gcm^{-3})	Grain size/ μm Para Perp	Thermal diffusivity/ (m^2s^{-1}) Para Perp	Thermal conductivity/ ($Wm^{-1}K^{-1}$) Para Perp	Lattice oxygen/%
La_2O_3	1.06	4	3.351	N/A N/A	0.12 0.13	28.1 31.6	0.2794±0.0371
		16	3.327	1.38 1.27	0.22 0.28	51.1 64.9	0.1163 ± 0.0055
Nd_2O_3	1.00	4	3.396	1.24 0.85	0.27 0.34	64.1 81.6	0.0942±0.0045
		16	3.379	2.39 2.06	0.31 0.41	72.2 97.9	0.0923±0.0134
Gd_2O_3	0.94	4	3.421	4.14 3.78	0.33 0.42	78.7 100.7	0.0692±0.0126
		16	3.420	4.74 4.00	0.34 0.45	81.6 106.9	0.0765±0.0013
Y_2O_3	0.89	4	3.252	4.58 4.16	0.36 0.46	82.9 104.6	0.0765±0.0013
		16	3.277	4.79 4.25	0.36 0.46	82.7 105.8	0.0632±0.0018
Yb_2O_3	0.86	4	3.462	3.85 3.73	0.36 0.47	86.1 115.0	0.0615±0.0022
		16	3.442	3.94 3.64	0.37 0.48	88.6 114.7	0.0802±0.0065
Sc_2O_3	0.73	4	3.231	3.61 3.46	0.38 0.45	84.9 100.8	0.0851±0.0038
		16	3.198	4.57 4.44	0.40 0.47	89.6 106.3	0.0775±0.0035

A number of studies have been made focusing on the lattice oxygen content in α-Si_3N_4 with values, ranging from 0.05 to 0.3 mass% for pure α-Si_3N_4 synthesized by chemical vapor deposition (CVD), and from 0.48 to 2 mass% for a-phase-rich Si_3N_4 (α-phase content 80%) [24]. Using various Y_2O_3/SiO_2 additive ratios Kitayama et al. investigated the relationship between thermal conductivity and lattice oxygen content for dense β-Si_3N_4 ceramics fabricated by hot-pressing and subsequent annealing. The thermal conductivity of β-Si_3N_4 crystals in the sintered specimens was estimated using a modification of the Wiener method in order to exclude microstructural factors such as grain size and the number of grain boundaries [39]. The inverse of thermal conductivity i. e. thermal resistivity of the β-Si_3N_4 crystal, increase in line with increases in the lattice oxygen content is confirmed by the results. This group of authors [24] used a hot-gas extraction method to determine the oxygen content in β-Si_3N_4 crystal lattices that originally had been developed for measuring the lattice oxygen in an AlN crystal [40]. Crystals of β-Si_3N_4 were fabricated using 15 mol% Y_2O_3–SiO_2 as additives (Y_2O_3:SiO_2 1 : 2 or 2 : 1) by heat treatment of α-Si_3N_4 as a raw powder followed by an acid rinse treatment to remove any secondary phases. Depending on the composition of the liquid phase the lattice oxygen contents in the β-Si_3N_4 crystal were reported as 0.258 mass% (in the case of Y_2O_3:SiO_2 1 : 2) and 0.158 mass% (in the case of Y_2O_3: SiO_2 2:1). Performance of thermal conduction would be expected to be lower due to the dissolution of oxygen into the β-Si_3N_4 a large number of lattice vacancies is formed leading to phonon scattering.

Secondary phases in Si_3N_4 ceramics formed after sintering, from the liquid phase remaining in the corners of or along the matrix grains as a thin film in addition to the lattice oxygen content, negatively affects the thermal conductivity to some extent. Thermal conductivities of these phases are 1–2 orders of magnitude lower than pure Si_3N_4 crystals like of yttrium aluminate (typical secondary phase in AlN with Y_2O_3 addition) and oxynitride glass (typical secondary phase in Si_3N_4) are about 10 $Wm^{-1}K^{-1}$ and 1 $Wm^{-1}K^{-1}$. Morphology distribution as a continuous film around the matrix grains substantially lowers the thermal conductivity, while isolated distribution in a form of pockets does not distinctly affect the thermal conductivity.

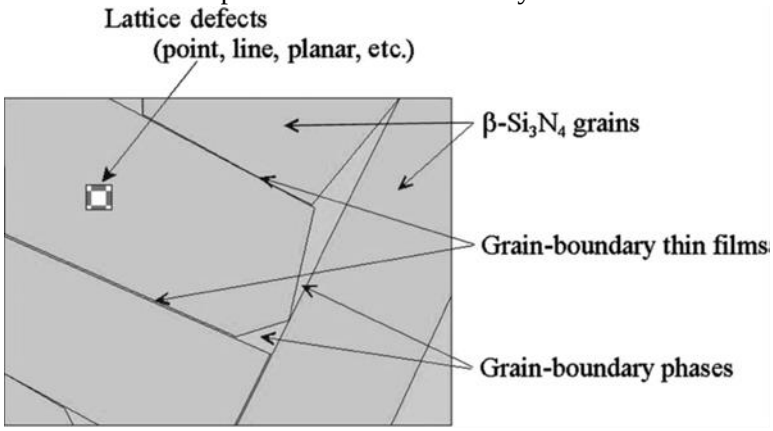

Figure 2. Microstructural factors of Si_3N_4 ceramic affecting thermal conductivity [9].

Owing to the well-faceted grains with a rodlike shape, microstructure of Si_3N_4 ceramic is more complicated, as illustrated in Figure 2. Secondary phase is generally presented as a glassy phase surrounding the matrix grains, mostly because of the liquid phase contains SiO_2 which is difficult to crystallize perfectly.

Glass has the thermal conductivity that can be as low as 1 $Wm^{-1}K^{-1}$, which is about one order of magnitude lower than the thermal conductivity of the crystalline secondary phase. Negative effect of the secondary phase on thermal conductivity is more pronounced in Si_3N_4 ceramic since distribution of glassy phase is not only as pockets surrounded by β-Si_3N_4 grains, but also in the openings between two grains as most of rodlike β-Si_3N_4 grains incline toward each other. Because β-Si_3N_4 grains have prismatic planes and are inclined to each other in most parts grain-boundary thin films present between two-grain junctions with an equilibrium thickness (typically 1–2 nm) [41] the other parts should have greater inter-grain in liquid-phase-sintered Si_3N_4 ceramic. The thermal conductivity of β-Si_3N_4 ceramic having grain-boundary films of a few nanometers' thickness decreases quickly as the size of the β-Si_3N_4 grains decreases to less than 1 μm according to calculation based on a simple modified Wiener's model [42] for the thermal conductivity of a composite material [39]. Calculation of the effect of the volume fraction of the glassy phase on the thermal conductivity of Si_3N_4 ceramics, with the aspect ratio of Si_3N_4 being 1, is illustrated in Figure 3. The calculation indicated that thermal conductivity of the β-Si_3N_4 crystal and the and the glassy phase if grain boundary thickness, δ, was 1 and 10 nm, were 180 and 1Wm^{-1} K^{-1}, respectively.

So, the thermal conductivity of Si_3N_4 ceramic is heavily dependent on the average grain boundary film thickness, which was in the range of a few tenths of a nanometer. When the grain boundary thickness was 1 nm the thermal conductivity of Si_3N_4 initially increased steeply with increasing grain size up to certain extent, to reach constant values determined by the film thickness and the amount of glassy phase. When the grain size exceeds certain critical values (about 1μm), grain-boundary thin films have little effect on the thermal conductivity of Si_3N_4, as shown in Figure 3. As for now, in addition to the role of purifying the β-Si_3N_4 lattice, grain growth is necessary in order to improve the thermal conductivity of Si_3N_4 ceramic.

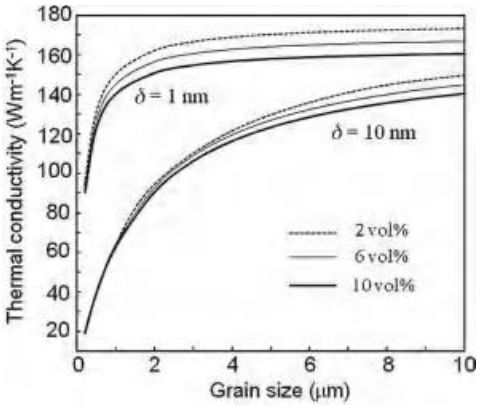

Figure 3. Effect of volume fraction of glassy phase on thermal conductivity of β-Si_3N_4 for R (aspect ratio)=1 in β-grain and δ=1 and 10 nm [2].

2.3. Improvements in Thermal Conductivity for Silicon Nitride Ceramics

One of the way improve the thermal conductivity for silicon nitride ceramics, is increasing sintering time in order to a reduce number of two-grain junctions [22,39], but also to the purification of grains [15] as a result of grain growth via solution–reprecipitation processes. A variation of sintering additives were used for improvement of Si_3N_4 thermal conductivity doped with 2 mol% MgO–5mol% Yb_2O_3 [43] by Hayshi, or with 1mass% HfO_2–8mass% Y_2O_3 [18] by Yokota after sintered at 2273K for between 2 and 48h. In order to exclude the effect of any α-phase → β-phase transformation in both experiments, β-Si_3N_4 were used as a raw powder. The thermal conductivities were increased during heating with increasing sintering time as a consequence of appreciable grain growth and decrease in lattice oxygen content in the β-Si_3N_4 grains [43]. Yokota et al. [18] with his experiments in which Si_3N_4 doped with HfO_2–Y_2O_3 additives was sintered at 2273 K for 8 and 48 h, obtain materials with increased thermal conductivities of 88 and 120$Wm^{-1}K^{-1}$. A bimodal microstructure where larger elongated grains with a grain diameter in excess of 2 μm were dispersed in fine matrix grains were obtained in both specimens. As expected, specimen sintered for 48 h had higher volume fraction of the larger grains compared to the specimen sintered for 8h. Why grain growth is so important regarding amount of impurity oxygen is experimentaly confirmed, a minimal change in lattice oxygen content of the smaller matrix grains was mesured between 8 and 48h (1900 ppm for 8h and 1920 ppm for 48 h). There was a drastic decrease in contrast in the lattice oxygen content of larger, elongated grains (980 ppm for 8h and 460 ppm for 48h).

Due to a higher affinity for oxygen in Y_2O_3 containing oxynitride glassy phase, the purification of β-Si_3N_4 grains occurs through a dissolution–reprecipitation process during long-term heating. Thus, the thermal conductivity of Si_3N_4 ceramic was increased with increasing amounts of purified larger grains [18].

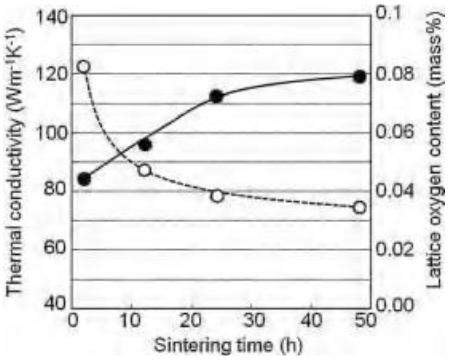

Figure 4. Variation of thermal conductivity and lattice oxygen content with sintering time for the Si_3N_4 specimens doped with 2 mol%MgO–5 mol% Yb_2O_3 sintered at 2173 K under 0.9 MPaN_2 [2]**.**

As already mentioned, one of the dominant extrinsic factors governing the high thermal conductivity of Si_3N_4 ceramics there is a clear tendency for thermal resistivity tends to decrease with a decreasing lattice oxygen content in the β-Si_3N_4 though the additive system, type of raw Si_3N_4 powder and processing method, were different among mentioned investigations (fig. 4). Literature data showed that the β-Si_3N_4 free of lattice oxygen exhibit a thermal conductivity of at least 180$Wm^{-1}K^{-1}$. Rare-earth oxides are well known as effective additives for preparing high-thermal conductivity Si_3N_4 [9,29]. Investigating the effect of rare-earth oxides (La, Nd, Gd, Y, Yb, and Sc) on the thermal conductivity hot-pressed α-Si_3N_4 powder, followed by subsequent annealing Kitayama et al. [37] showed that with a decreasing ionic radius of the rare-earth element, the mean grain size was increased while the lattice oxygen was decreased, and hence the thermal conductivity was increased. Because there is a close connection between the grain growth and oxygen removal, the obtained results of these experiments could not confirm which factor microstructure or lattice oxygen has dominant influence on thermal conductivity. However, it was concluded based on the obtained results, that the type of rare-earth oxide additive had a significant influence on the thermal conductivity of β-Si_3N_4, since it depends on ionic radius (table 1). As it was already mentioned, the ratio of additive oxide to SiO_2 existing in a raw Si_3N_4 powder would also affect the thermal conductivity of the sintered specimens showing tendency to increase with increasing Y_2O_3:SiO_2 ratio, with a significant rise occurring when the ratio was close to 1 by Kitayama et al. [25]. He fabricated Si_3N_4 with various Y_2O_3/SiO_2 additive ratios (0.289, 0.807, 1.267, and 2.029) by hot-pressing. The same effect occurring with Y_2O_3-doped AlN proposed by Jackson et al. [44] explaines the effect of grain-boundary composition on the thermal conductivity of Y_2O_3-doped Si_3N_4. There is a three-phase field with an increasing Y_2O_3:SiO_2 ratio, shifting from region I (Si_3N_4–Si_2N_2O–$Y_2Si_2O_7$), to region II (Si_3N_4-$Y_2Si_2O_7$–$Y_{20}N_4Si_{12}O_{48}$), and finally to region III (Si_3N_4–$Y_{20}N_4Si_{12}O_{48}$–$Y_2Si_3N_4O_3$). The activity of SiO_2 was decreased in the order of regions I, II, and III in corresponding with the variant of the three-phase field. In this case, So, the lattice oxygen content of β-Si_3N_4, depending on the activity of SiO_2 dictated the grain-boundary phase composition in the three-phase field.

The solubility of oxygen in β-Si_3N_4 was the lower as the the activity of SiO_2 was lower in the three-phase field. When both the $Y_{20}N_4Si_{12}O_{48}$ and $Y_2Si_3N_4O_3$ phases were present in the grain-boundary phase simultaneously, the highest thermal conductivity was achieved.

One of the effective ways of improving the thermal conductivity of Si_3N_4 considering the amount of oxygen in the grain-boundary glassy phase, is to use of a nitride sintering additive. Hayashi et al. [43] measured the lattice oxygen content of the β-Si_3N_4 grains and thermal conductivity in compacts of β-Si_3N_4 raw powder doped with either MgO–Yb_2O_3 or $MgSiN_2$–Yb_2O_3 as an additives, sintered at 2273 K for 2 to 48h under a 0.9MPa nitrogen pressure. Specimen in which $MgSiN_2$ was used as additive a magnesium supply source exhibited a lower lattice oxygen content, and thus a higher thermal conductivity for about 20$Wm^{-1}K^{-1}$ higher than that of the MgO-doped Si_3N_4, and reached a maximum of over 140W $m^{-1}K^{-1}$ following a 48h period of sintering. Enhanced grain growth that had resulted in a microstructure where the larger grains were in contact with each other and the purification of Si_3N_4 grains via a solution–reprecipitation process in the nitrogen-rich grain boundary glassy phase was provided by MgS_iN_2 as non-oxide additive and as consequence higher thermal conductivity Si_3N_4. Thus, a key approach to improving the thermal conductivity of Si_3N_4 ceramics is to remove the lattice oxygen by using high purity β- Si_3N_4 or Si raw materials with effective sintering additives and high-temperature sintering/annealing processes. In order to achieve improved thermal conductivities, over 100 W $m^{-1}K^{-1}$ in untextured Si_3N_4, where elongated β-Si_3N_4 grains are randomly aligned much effort has been made [15,22,26,45–47] . An untextured Si_3N_4 was reported by Zhou et al.[48] having thermal conductivity of 177 W $m^{-1}K^{-1}$ obtained by sintering reaction-bonded Si_3N_4 (RBSN) at 1900◦C for 60 h, followed by cooling at a very low rate of 0.2◦C min^{-1}. Since the thermal conductivity of β-Si_3N_4 is intrinsically anisotropic with a thermal anisotropy as high as 450/170 (thermal conductivity along c and a-axis) = 2.6. A self-reinforced Si_3N_4 ceramic with high thermal conductivity was prepared by Kong et al. [49] through multi-step pressureless sintering with Y_2O_3 and MgO additives. The steps consisted of phase control and densification stages to provide additional crystallization sites using a partial α-β phase transformation, which also established a bimodal microstructure. In the case of specimen (first-step temperature of 1400 °C), the best mechanical and thermal properties were obtained, flexural strength 932 MPa and thermal conductivity of 74 $W/m^{-1}K^{-1}$. This can be attributed to the specific phase transformation and linear shrinkage that occurred at this condition.

2.4. Harmonic Improvement of Thermal Conductivity and Mechanical Properties

The relationship between grain size and thermal conductivity can be established by considering the calculated phonon mean free path for the sintered materials. If the phonons are scattered significantly by the presence of grain boundary, the phonon mean free path must equal the magnitude of the grain size. However, the grains of the samples were too large compared with the phonon mean free path. Hence, the thermal conductivity of Si3N4 ceramics must not be controlled by the grain size. Thermal conductivities of the samples were enhanced as the frequencies of the large grains increased. The relationship between grain size and thermal conductivity can be established by considering the calculated phonon mean free path for the sintered materials. If the phonons are scattered significantly by the presence of grain boundary, the phonon mean free path must equal the magnitude of the grain size. However, the grains of the samples were too large compared with the phonon mean free path. Hence, the thermal conductivity of Si3N4 ceramics must

not be controlled by the grain size. Thermal conductivities of the samples were enhanced as the frequencies of the large grains increased [50]. Enhance grain growth of β-Si_3N_4 grains throughout dissolution–reprecipitation process decreases the lattice oxygen thus leading to improved thermal conductivity of Si_3N_4 ceramicis. Grain growth further participates in reducing the number of grain boundary glassy phases between two β-Si_3N_4 grains and increase thermal conductivity of Si_3N_4.

Approach set in this way is only beneficial for a critical value of grain size, below a few microns [39]. In order to achieve grain purification, gas-pressure sintering is common way for fabrication of high-thermal conductivity (>100Wm-1K-1) Si_3N_4 ceramics at temperatures of about 2173 K for anunusually long period of time (1–2 days), or at temperatures in excess of 2373K under high N2 pressures (>10MPa) for several hours [51]. Obtained material, however, has very poor mechanical properties originated from coarse microstructure.

2.5. High Thermal Conductivity Through Reaction Bonding and Post Sintering

Another approach to over come this problem is to apply a reaction bonding (RB) process. Silicon nitride ceramics from a Si powder compact are ussualy fabricate this way [52]. Reducing the impurities in raw silicon powder to an extremely low level was noted in 1995 by Haggerty et al. Leading to that improved thermal conductivity of reaction-bonded Si_3N_4 [53]. High-thermal conductivity silicon nitrides by sintering of reaction-bonded silicon nitride (RBSN) were investigated by a research group at the National Institute of Advanced Industrial Science & Technology, in Japan [2,51,54–56]. A silicon nitride compact is formed when a Si powder compact is heated at about 1673K in a nitrogen atmosphere. The external dimensions of the compact are retained as the individual Si particles expands by about 22 %, and nitridation reaction proceeds (mainly via a gas–solid reaction system) [52]. Reaction bonding process offers following improvements: (1) rather than the more expensive Si_3N_4 powder a cheaper Si powder can be used as the starting material, (2) because of the higher density of the pre-sintered specimens shrinkages accompanied by post-sintering can be minimized. Starting with the pre-sintered specimen with a finer microstructure and a higher density which favorable for controlling the microstructure of the final product RB process provides fabricating high-performance silicon nitride ceramics.

The reaction bonding and post sintering has been known as a fabrication process of dense silicon nitride sintered body where Si powder compact is heat-treated in nitrogen atmosphere for transformation into Si_3N_4 and post-sintered [52,57] . For full densification by this approach, the nitridation and post-sintering are carried out in an inert atmosphere, leading to substantial reduction in the impurity oxygen content [57]. Furthermore, even coarse Si powder is decomposed into fine Si3N4 powder in nitridation as shown, thus facilitating full densification during the post sintering [51,55,57]. As starting, raw powder a high purity Si powder with an oxygen content of 0.28 wt%, a total metallic impurity content of <0.01 wt%, and a mean particle size (d50) of 50 8.5 μm was used. As sintering additives during post-sintering high purity 2 mol%Y2O3 - 5 mol%MgO were added to the Si powder, and were mixed in methanol using a planetary mill. The oxygen content of Si powders after planetary milling increased to 0.51 wt% (from 0.28 wt%), which was still relatively low compared to those of the commercial high-purity Si3N4 powders (typically 1 wt% or higher). Sintered reaction-bonded silicon nitride (SRBSN) which was obtained through reaction-bonding (nitridation) at 1400°C for 8 h under 0.1 MPa nitrogen pressure and post-sintering at 1900°C for

12 h under 0.9 MPa nitrogen pressure had large fibrous grains embedded in fine grain matrix without pores. For comparison, microstructure of gas-pressure sintered silicon nitride (GPSSN) obtained under the same sintering conditions using a commercial high-purity Si3N4 powder (mean particle size: 0.2 μm, oxygen content: 1.2 wt%).

Although similar microstructures, the thermal conductivity of the SRBSN is 120 W/(m·K), which was about 20% higher than that of the GPSSN, 98 W/(m·K), due to a smaller amount of impurity oxygen contained in the starting powder. So, it was confirmed that with increasing the sintering time, the thermal conductivity increases for all the samples due to grain coarsening and diffusion of lattice oxygen into grain boundaries [58]. Also, the SRBSN shows both high strength and high thermal conductivity compared to the GPSSN . Zhou, et al. [58]investigated in detail the effects of nitridation conditions on the properties of the nitrided and post-sintered samples, and revealed that further improvement of the thermal conductivity is possible by increasing β/α phase ratio of the nitrided sample from conventional 60:40 to 83:17 via controlling the nitrogen atmosphere in the nitridation (the modified SRBSN). Due to further reduced content of impurity oxygen in the post-sintered sample derived from the nitrided sample of high β phase ratio, since it is known that an amount of oxygen solved into β-Si3N4 is smaller than that into α-Si3N4.

Lowered thermal conductivity due to the content of lattice oxygen, could be reduced also by enhanced grain growth via a solution–reprecipitation process not only by reaction with sintering additives to form stable compounds at the grain boundaries. Thermal conductivity of β-Si_3N_4 ceramics is affected by microstructural factors the, such as porosity, grain size (particularly large elongated grain size) [59]. Zhu et al. [55] investigated the effect of the impurity oxygen content of raw Si powder on the properties of a RBSN ceramic using A (finer) and B (coarser) powder. But these microstructure factors are not responsible for the difference in the thermal conductivity between the A (finer) and B (coarser) powder samples, owing to the following facts: (i) the former shows more complete densification than the latter; (ii) the former shows more pronounced large elongated β-Si_3N_4 grain growth than the latter, which is inconsistent with the previous reports that the thermal conductivity of β-Si_3N_4 ceramics increases with increased fraction of large grains as a result of the increased contiguity of β-Si_3N_4–β-Si_3N_4 [17,18,22,43,60,61] and (iii) although the former shows a slightly higher amount of secondary phases than the latter, the secondary phases in both the samples are predominantly located at the triple grain–boundary junction. This distribution makes the secondary phases less harmful to the thermal conductivity of β-Si_3N_4 ceramics [16]. Therefore, the reason why the B (coarser) powder sample shows higher thermal conductivity than the A (finer) powder sample is mainly attributed to fewer lattice defects in the former, due to the lower native oxygen content and the least level of aluminum impurity from the raw powder. It is of interest to see that there is no difference in the thermal conductivity between the A powder samples sintered from the nitrided bodies at 1350°C and 1400°C, suggesting that the nitriding temperature has no effect on the thermal conductivity of SRBSN. On the one hand, the nitriding temperature does not affect the β-Si_3N_4 grain growth via a solution–reprecipitation process during post-sintering, so it most likely does not affect the removal of lattice oxygen in β-Si_3N_4. On the other hand, considering that the dissolved Al in β-Si_3N_4 is stable during sintering, it is believed that the nitriding temperature has no effect on the removal of the dissolved Al in β-Si_3N_4 during post sintering. As a result, the same thermal conductivity is due to the similar microstructure as well as the similar lattice defects between them. It is interesting to see that the thermal conductivity of the SSN material appears

almost the same as that of the SRBSN material but is lower than that of the SRBSN material prepared from B (coarser) powder.

This is because the high-purity coarse Si powder with several micrometers, even with a few tenths of a micrometer, is feasible for producing dense SRBSN materials, which is beneficial for further reducing the cost of production, because the nitridation makes them convert into sub-microsized and even nanosized Si_3N_4 products [62,63]. From the stand point of enhancing the thermal conductivity of SRBSN, the present work suggests that further decreasing the particle size is unnecessary for the following reasons. (i) The prolonged milling process invariably introduces greater amounts of both extraneous aluminum impurity and oxygen, which may be detrimental to thermal conductivity of SRBSN (ii) Complete nitridation can be achieved at a temperature of 1400°C, near the melting point of Si. The property evaluation reveals that the coarse Si powder leads to a higher thermal conductivity of SRBSN than the fine Si powder, which is attributed to the lower amounts of native oxygen and aluminum impurities. However, the nitriding temperature has no effect on the thermal conductivity of SRBSN and this is in agreement with the similar microstructure as well as the similar lattice defects. This work demonstrates that the improvement in high thermal conductivity of SRBSN materials could be achieved by using a coarse Si powder with lower amounts of native oxygen and aluminum impurity.

2.6. Anisotropic Thermal Conductivity in Textured Si_3N_4

Due to its strong intrinsic thermal anisotropy the formation of a textured microstructure is necessary to obtain Si_3N_4 ceramics with high thermal conductivities. Control of the amount of oxygen impurity which depend on the sintering additives and the degree of texture depending on texturing method used, is decisive to enhance the thermal conductivity of textured Si_3N_4, respectively [47,64]. Development of textured microstructure in which the elongated β-Si_3N_4 grains are oriented almost unidirectionally as shown in figure 5 is another approach to achieve a high thermal conductivity in Si_3N_4 ceramic. Because of the much higher thermal conductivity along the c-axis than along the a-axis in β-Si_3N_4 crystals a high thermal conductivity along the grain orientation would be expected, compared to a material with a random distribution of β-Si_3N_4 grains [65,66]. Forming process generating shear stress, such as tape-casting and extrusion in a combination of the seeding of rod-like β-Si_3N_4 nuclei and a enables fabrication of anisotropic microstructures [67–69]. This process is based on the grain-growth behavior of silicon nitride during the α-to β-phase transformation, with the preferential nucleation site of the newly formed β-Si_3N_4 phase on pre-existing β particles. After the transformation only few α and large β grains will be distributed selectively particularly along the c-axis direction, via a solution–reprecipitation reaction. The typical microstructure of seeded and extruded Si_3N_4 is shown in Figure 5 [2,70]. The method of adding large β-Si_3N_4 grains to the raw Si_3N_4 powder by grain growth of Si_3N_4 crystals in polycrystalline ceramics improves thermal conductivity due to purification of the grains while decreasing the two-grain junction films. Introducing large β -Si_3N_4 particles as seeds into fine Si_3N_4 raw powder is effective in controlling the microstructure. During firing, fine Si_3N_4 dissolves and precipitates on the large β -Si_3N_4 particles. Seeds addition accelerates grain growth because the driving force for grain growth is the diference in grain size. Seeds addition increased the thermal conductivity up to 106 $Wm^{-1}K^{-1}$, under the condition of heat-treatment at 2000°C, thermal conductivity increased up to 122 $Wm^{-1}K^{-1}$. Grain growth not only decreases the amount of films, but also purifies the impurities and defects in the

Si_3N_4 grains because silicon nitride raw powders contain impurities and crystal defects in the grain. The grown parts of Si_3N_4 grain have a lower amount of impurities and defects than the raw Si_3N_4 powder because most of impurities and defects in the raw powder are removed by the segregation phenomena at the precipitation step during the liquid phase sintering in which smaller Si_3N_4 grains dissolve to the liquid, difuse in the liquid, and reprecipitate onto the larger grains. Therefore, the material with large grain size has higher thermal conductivity [71]. (N. Hirosaki et al., Journal of the European Ceramic Society 19 (1999) 2183-2187).

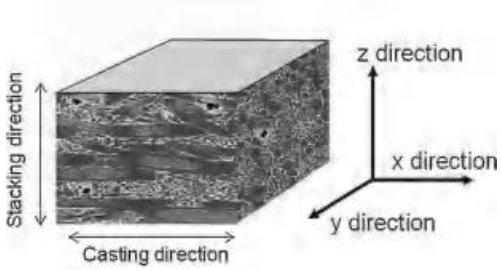

Figure 5. Microstructure of seeded and tape-cast Si_3N_4 (left-hand side) and three different directions for thermal conductivity measurements (right-hand side) [2,59]

The material exhibits a high anisotropy where the large elongated grains, which are grown from seeds, are almost unidirectionally oriented parallel to the forming process which is used. The thermal conductivities are measured in three different directions (as shown in fig. 4) [9]. As expected, for each of these specimens the thermal conductivity was highest along the grain alignment. In particular, a highly anisotropic Si_3N_4 with very long grains and fabricated under extreme conditions, exhibited a high thermal conductivity of about 150 $Wm^{-1}K^{-1}$ in the direction parallel to the grain alignment [69]. In recent times, futher improvements are made considering fabricatinion of textured silicon nitride. Fabrication of textured Si_3N_4 with the c-axis parallel to the thickness direction is also feasible with Strong Magnetic Field (SMFA). Highly textured ceramics by colloidal processing can be simply obtain in a strong magnetic field Strong Magnetic Field. As confirmed by Sakka et al. [72,73]. Zhu et al. [74] using highly c-axis-textured Si_3N_4 a highly textured Si_3N_4 ceramics was produced, with a thermal anisotropy of 2.2 by seeded slip casting in a rotating strong magnetic field (RSMF). Zhu et al. [47,64,74] propose a strategy for fabricating textured Si_3N_4 with high thermal conductivity of over 170 W $m^{-1}K^{-1}$ along the grain alignment direction by slip casting α-Si_3N_4 raw powder with β-Si_3N_4 seeds and Y_2O_3–$MgSiN_2$ [45] as sintering additives in an RSMF in a rotating strong magnetic field of 12 T, followed by gas pressure sintering at 1900°C for 12 h at a nitrogen pressure of 1 Mpa. Yang et al. [75] fabricated high thermal conductive β-silicon nitride (β-Si_3N_4) ceramics from fine α-Si_3N_4 powder as the raw material and coarse β-Si_3N_4 particles as the nuclei through spark plasma sintering (SPS) at 1650 °C for 5 min and post-sintering heat treatment at 1900 °C for 4 h. The thermal conductivity of the sample with 10 mol% of β-Si_3N_4 nuclei reached a maximum value of 84.6 W/mK. These results revealed that the thermal conductivity of β-Si_3N_4 ceramics was independent of the grain size and controlled by the amount of reprecipitated large grains. Strong magnetic field alignment (SMFA) is a novel and potential technique for the near-net-shape production of textured ceramics. In addition, it has no limitations to the particle morphology of the raw powder. This technique has two key requirements: (i) the material should exhibit the magnetic anisotropy, normally with a noncubic crystal structure and (ii) the suspension should be well

deagglomerated to allow the orientation of single crystals [72]. A rotating strong magnetic field (RSMF) is one solution to achieve the c-axis orientation, and this is practically conducted by rotating the sample in a horizontal static strong magnetic fiel (SSMF) and has been used to produce c-axis textured ceramics such as Si_3N_4 [64]. The anisotropic properties result from the orientation of elongated β-Si_3N_4 grains or its combination with intrinsic anisotropic properties of β-Si_3N_4. The intrinsic thermal conductivity (ideal crystal: 170 (a-axis) and 450 $W/m^{-1}\cdot K^{-1}$ (c-axis) [65] allows the texturing to efficiently improve thermal conductivity of Si_3N_4 ceramics [70]. Zhu et al. [74] investigate the c-axis texture development and thermal conductivity in seeded Si_3N_4 with β-Si_3N_4 whiskers by slip casting in an RSMF. The thermal conductivity in the directions parallel and perpendicular to the slip casting direction, corresponding to 29 and 30 W/m·K respectively, indicating the thermal isotropy. However, the c-axis oriented sample exhibits 25 and 51 W/m·K in the directions parallel and perpendicular to the rotating magnetic field, i.e., perpendicular and parallel to the c-axis of β-Si_3N_4 grains.

3. Summary and outlook

Amounts of lattice oxygen and grain boundary phase, textured Si_3N_4 as the most important factors affecting the thermal conductivity of silicon nitride ceramics were reviewed in in this paper. Much research has been carried out in order to improve thermal conductivity using of variety of production methods. This review has mainly focused on the effects of sintering additives and the forming and sintering processes on the thermal conductivity of silicon nitride ceramics. Some clear conclusions can be draw summarizing the presented research results,: (1) the addition of non-oxide sintering additives tends to improve the thermal conductivity of silicon nitride ceramics comparing to oxide sintering additives; (2) the growth of β-Si_3N_4 grains is promoted with increase in sintering temperature and holding time, and the oxygen content of the crystal lattice is continuously reduced by the process of dissolving-precipitate, thereby promoting the increase of thermal conductivity; (3) the orientation of β- Si_3N_4 grains in textured Si_3N_4 ceramics affects the thermal conductivity of silicon nitride ceramics in different directions parallel and perpendicular to the grain alignment. For practical use of highly-thermal-conductive Si_3N_4 ceramic, many problems still need to be solved, like development of low-cost technology. Currently used preparation methods are longtime while heat treatments at high temperatures require high energy consumption and long cycle times and are, therefore, expensive. Special attention for the future research should be paid on how to control the effects of lattice oxygen and grain boundary phases at lower temperatures and shorter holding times and how to reduce the sintering temperature. Finally, development of high thermal conductivity of silicon nitride ceramics should correlate with improved mechanical properties.

Acknowledgment

The authors would like to thank Ministry of Science, Technological Development and Innovation of the Republic of Serbia for financial support under Grant No. 451-03-68/2022-14/200017 and 451-03-47/2023-01/200051.

References

[1] R. Grün, The crystal structure of β-Si\sb 3N\sb 4: structural and stability considerations between α- and β-Si\sb 3N\sb 4, Acta Crystallographica Section B 35 (1979) 800–804. https://doi.org/10.1107/S0567740879004933.

[2] R. Riedel, I.-W. Chen, eds., Ceramics science and technology, Wiley-VCH, Weinheim, 2008.

[3] A. Zerr, G. Miehe, G. Serghiou, M. Schwarz, E. Kroke, R. Riedel, H. Fueß, P. Kroll, R. Boehler, Synthesis of cubic silicon nitride, Nature 400 (1999) 340–342. https://doi.org/10.1038/22493.

[4] F.L. Riley, Silicon Nitride and Related Materials, Journal of the American Ceramic Society 83 (2000) 245–265. https://doi.org/10.1111/j.1151-2916.2000.tb01182.x.

[5] C. Alexander, C. Prombo, P. Swan, R. Walker, SiC, and Si3N4 in Qingzhen (EH3), in: 1991.

[6] C.M.O. Alexander, P. Swan, C.A. Prombo, Occurrence and implications of silicon nitride in enstatite chondrites, Meteoritics 29 (1994) 79–85. https://doi.org/10.1111/j.1945-5100.1994.tb00656.x.

[7] J. Stone, I.D. Hutcheon, S. Epstein, G.J. Wasserburg, Correlated Si isotope anomalies and large13C enrichments in a family of exotic SiC grains, Earth and Planetary Science Letters 107 (1991) 570–581. https://doi.org/10.1016/0012-821X(91)90102-N.

[8] M.R. Lee, S.S. Russell, J.W. Arden, C.T. Pillinger, Nierite (Si3N4), a new mineral from ordinary and enstatite chondrites, Meteoritics 30 (1995) 387–398. https://doi.org/10.1111/j.1945-5100.1995.tb01142.x.

[9] K. Hirao, K. Watari, H. Hayashi, M. Kitayama, High Thermal Conductivity Silicon Nitride Ceramic, MRS Bull. 26 (2001) 451–455. https://doi.org/10.1557/mrs2001.115.

[10] N.P. Padture, *In Situ* -Toughened Silicon Carbide, Journal of the American Ceramic Society 77 (1994) 519–523. https://doi.org/10.1111/j.1151-2916.1994.tb07024.x.

[11] F.F. Lange, Fracture Toughness of Si_3N_4 as a Function of the Initial α-Phase Content, Journal of the American Ceramic Society 62 (1979) 428–430. https://doi.org/10.1111/j.1151-2916.1979.tb19096.x.

[12] G.A. Slack, Nonmetallic crystals with high thermal conductivity, Journal of Physics and Chemistry of Solids 34 (1973) 321–335. https://doi.org/10.1016/0022-3697(73)90092-9.

[13] G.A. Slack, R.A. Tanzilli, R.O. Pohl, J.W. Vandersande, The intrinsic thermal conductivity of AIN, Journal of Physics and Chemistry of Solids 48 (1987) 641–647. https://doi.org/10.1016/0022-3697(87)90153-3.

[14] X. Zhu, H. Hayashi, Y. Zhou, K. Hirao, Influence of additive composition on thermal and mechanical properties of β–Si_3N_4 ceramics, J. Mater. Res. 19 (2004) 3270–3278. https://doi.org/10.1557/JMR.2004.0416.

[15] X. Zhu, Y. Zhou, K. Hirao, T. Ishigaki, Y. Sakka, Potential use of only Yb_2O_3 in producing dense Si_3N_4 ceramics with high thermal conductivity by gas pressure sintering, Science and Technology of Advanced Materials 11 (2010) 065001. https://doi.org/10.1088/1468-6996/11/6/065001.

[16] J.-M. Kim, S.-I. Ko, H.-N. Kim, J.-W. Ko, J.-W. Lee, H.-D. Kim, Y.-J. Park, Effects of microstructure and intergranular glassy phases on thermal conductivity of silicon nitride, Ceramics International 43 (2017) 5441–5449. https://doi.org/10.1016/j.ceramint.2017.01.037.

[17] H. Yokota, M. Ibukiyama, Effect of lattice impurities on the thermal conductivity of β-Si3N4, Journal of the European Ceramic Society 23 (2003) 55–60. https://doi.org/10.1016/S0955-2219(02)00074-2.

[18] H. Yokota, S. Yamada, M. Ibukiyama, Effect of large β-Si3N4 particles on the thermal conductivity of β-Si3N4 ceramics, Journal of the European Ceramic Society 23 (2003) 1175–1182. https://doi.org/10.1016/S0955-2219(02)00291-1.

[19] M. Kitayama, K. Hirao, A. Tsuge, M. Toriyama, S. Kanzaki, Oxygen Content in ß-Si3N4 Crystal Lattice, Journal of the American Ceramic Society 82 (1999) 3263–3265. https://doi.org/10.1111/j.1151-2916.1999.tb02238.x.

[20] C. Yang, Q. Liu, B. Zhang, J. Ding, Y. Jin, F. Ye, Z. Zhang, L. Gao, Effect of MgF2 addition on mechanical properties and thermal conductivity of silicon nitride ceramics, Ceramics International 45 (2019) 12757–12763. https://doi.org/10.1016/j.ceramint.2019.03.183.
[21] W. Dressler, R. Riedel, Progress in silicon-based non-oxide structural ceramics, International Journal of Refractory Metals and Hard Materials 15 (1997) 13–47. https://doi.org/10.1016/S0263-4368(96)00046-7.
[22] N. Hirosaki, Y. Okamoto, M. Ando, F. Munakata, Y. Akimune, Thermal Conductivity of Gas-Pressure-Sintered Silicon Nitride, Journal of the American Ceramic Society 79 (1996) 2878–2882. https://doi.org/10.1111/j.1151-2916.1996.tb08721.x.
[23] K. Watari, Y. Seki, K. Ishizaki, Temperature Dependence of Thermal Coefficients for HIPped Silicon Nitride, J. Ceram. Soc. Japan 97 (1989) 174–181. https://doi.org/10.2109/jcersj.97.174.
[24] M. Kitayama, K. Hirao, A. Tsuge, M. Toriyama, S. Kanzaki, Oxygen Content in ß-Si3N4 Crystal Lattice, Journal of the American Ceramic Society 82 (1999) 3263–3265. https://doi.org/10.1111/j.1151-2916.1999.tb02238.x.
[25] M. Kitayama, K. Hirao, A. Tsuge, K. Watari, M. Toriyama, S. Kanzaki, Thermal Conductivity of β-Si3N4: II, Effect of Lattice Oxygen, Journal of the American Ceramic Society 83 (2000) 1985–1992. https://doi.org/10.1111/j.1151-2916.2000.tb01501.x.
[26] H. Yokota, H. Abe, M. Ibukiyama, Effect of lattice defects on the thermal conductivity of β-Si3N4, Journal of the European Ceramic Society 23 (2003) 1751–1759. https://doi.org/10.1016/S0955-2219(02)00374-6.
[27] Y. Akimune, F. Munakata, K. Matsuo, N. Hirosaki, Y. Okamoto, K. Misono, Raman Spectroscopic Analysis of Structural Defects in Hot Isostatically Pressed Silicon Nitride., J. Ceram. Soc. Japan 107 (1999) 339–342. https://doi.org/10.2109/jcersj.107.339.
[28] N. Hirosaki, T. Saito, F. Munakata, Y. Akimune, Y. Ikuhara, Transmission electron microscopy observation of second-phase particles in β–Si3N4 grains, Journal of Materials Research 14 (1999) 2959–2965. https://doi.org/10.1557/JMR.1999.0396.
[29] K. Watari, High Thermal Conductivity Non-Oxide Ceramics., J. Ceram. Soc. Japan 109 (2001) S7–S16. https://doi.org/10.2109/jcersj.109.S7.
[30] Y. Okamoto, N. Hirosaki, M. Ando, F. Munakata, Y. Akimune, Effect of sintering additive composition on the thermal conductivity of silicon nitride, J. Mater. Res. 13 (1998) 3473–3477. https://doi.org/10.1557/JMR.1998.0474.
[31] Y. Lin, X.-S. Ning, H. Zhou, K. Chen, R. Peng, W. Xu, Study on the thermal conductivity of silicon nitride ceramics with magnesia and yttria as sintering additives, Materials Letters 57 (2002) 15–19. https://doi.org/10.1016/S0167-577X(02)00690-0.
[32] H.-J. Yeom, Y.-W. Kim, K.J. Kim, Electrical, thermal and mechanical properties of silicon carbide–silicon nitride composites sintered with yttria and scandia, Journal of the European Ceramic Society 35 (2015) 77–86. https://doi.org/10.1016/j.jeurceramsoc.2014.08.011.
[33] Y. Duan, J. Zhang, X. Li, H. Bai, P. Sajgalik, D. Jiang, High thermal conductivity silicon nitride ceramics prepared by pressureless sintering with ternary sintering additives, Int J Applied Ceramic Tech 16 (2019) 1399–1406. https://doi.org/10.1111/ijac.13220.
[34] T. Lu, T. Wang, Y. Jia, M. Ding, Y. Shi, J. Xie, F. Lei, L. Zhang, L. Fan, Fabrication of high thermal conductivity silicon nitride ceramics by pressureless sintering with MgO and Y2O3 as sintering additives, Ceramics International 46 (2020) 27175–27183. https://doi.org/10.1016/j.ceramint.2020.07.198.
[35] K. Watari, M.E. Brito, M. Toriyama, K. Ishizaki, S. Cao, K. Mori, Thermal conductivity of Y2O3-doped Si3N4 ceramic at 4 to 1000 K, Journal of Materials Science Letters 18 (1999) 865–867. https://doi.org/10.1023/A:1006696126661.

[36] H. Yokota, M. Ibukiyama, Microstructure Tailoring for High Thermal Conductivity of β-Si3N4 Ceramics, Journal of the American Ceramic Society 86 (2003) 197–199. https://doi.org/10.1111/j.1151-2916.2003.tb03305.x.
[37] M. Kitayama, K. Hirao, K. Watari, M. Toriyama, S. Kanzaki, Thermal conductivity of beta-Si(3)N(4): III, effect of rare-earth (RE = La, Nd, Cd, Y, Yb, and Sc) oxide additives, Journal of the American Ceramic Society 84 (2001) 353–358.
[38] M. Kitayama, K. Hirao, K. Watari, M. Toriyama, S. Kanzaki, Thermal conductivity of beta-Si(3)N(4): III, effect of rare-earth (RE = La, Nd, Cd, Y, Yb, and Sc) oxide additives, Journal of the American Ceramic Society 84 (2001) 353–358.
[39] M. Kitayama, K. Hirao, M. Toriyama, S. Kanzaki, Thermal Conductivity of ß-Si3N4: I, Effects of Various Microstructural Factors, Journal of the American Ceramic Society 82 (1999) 3105–3112. https://doi.org/10.1111/j.1151-2916.1999.tb02209.x.
[40] A. Thomas, G. Müller, Determination of the concentration of oxygen dissolved in the AlN lattice by hot gas extraction from AlN ceramics, Journal of the European Ceramic Society 8 (1991) 11–19. https://doi.org/10.1016/0955-2219(91)90087-G.
[41] H. Kleebe, M.K. Cinibulk, R.M. Cannon, M. Rüble, Statistical Analysis of the Intergranular Film Thickness in Silicon Nitride Ceramics, Journal of the American Ceramic Society 76 (1993) 1969–1977. https://doi.org/10.1111/j.1151-2916.1993.tb08319.x.
[42] V.R. Raghavan, H. Martin, Modelling of two-phase thermal conductivity, Chemical Engineering and Processing: Process Intensification 34 (1995) 439–446. https://doi.org/10.1016/0255-2701(94)00577-X.
[43] H. Hayashi, K. Hirao, M. Toriyama, S. Kanzaki, K. Itatani, MgSiN2 Addition as a Means of Increasing the Thermal Conductivity of β-Silicon Nitride, Journal of the American Ceramic Society 84 (2001) 3060–3062. https://doi.org/10.1111/j.1151-2916.2001.tb01141.x.
[44] T.B. Jackson, A.V. Virkar, K.L. More, R.B. Dinwiddie, R.A. Cutler, High-Thermal-Conductivity Aluminum Nitride Ceramics: The Effect of Thermodynamic, Kinetic, and Microstructural Factors, Journal of the American Ceramic Society 80 (1997) 1421–1435. https://doi.org/10.1111/j.1151-2916.1997.tb03000.x.
[45] X. Zhu, H. Hayashi, Y. Zhou, K. Hirao, Influence of additive composition on thermal and mechanical properties of β–Si_3N_4 ceramics, J. Mater. Res. 19 (2004) 3270–3278. https://doi.org/10.1557/JMR.2004.0416.
[46] X. Zhu, Y. Zhou, K. Hirao, Z. Lenčéš, Processing and Thermal Conductivity of Sintered Reaction-Bonded Silicon Nitride: (II) Effects of Magnesium Compound and Yttria Additives, Journal of the American Ceramic Society 90 (2007) 1684–1692. https://doi.org/10.1111/j.1551-2916.2006.01462.x.
[47] X.W. Zhu, Y. Sakka, Y. Zhou, K. Hirao, K. Itatani, A strategy for fabricating textured silicon nitride with enhanced thermal conductivity, Journal of the European Ceramic Society 34 (2014) 2585–2589. https://doi.org/10.1016/j.jeurceramsoc.2014.01.025.
[48] Y. Zhou, H. Hyuga, D. Kusano, Y. Yoshizawa, K. Hirao, A Tough Silicon Nitride Ceramic with High Thermal Conductivity, Advanced Materials 23 (2011) 4563–4567. https://doi.org/10.1002/adma.201102462.
[49] J.H. Kong, H.J. Ma, W.K. Jung, J. Hong, K. Jun, D.K. Kim, Self-reinforced and high-thermal conductivity silicon nitride by tailoring α-β phase ratio with pressureless multi-step sintering, Ceramics International 47 (2021) 13057–13064. https://doi.org/10.1016/j.ceramint.2021.01.169.
[50] K. Watari, K. Hirao, M. Toriyama, K. Ishizaki, Effect of Grain Size on the Thermal Conductivity of Si3N4, (n.d.).
[51] Y. Zhou, X. Zhu, K. Hirao, Z. Lences, Sintered Reaction-Bonded Silicon Nitride with High Thermal Conductivity and High Strength, Int J Applied Ceramic Tech 5 (2008) 119–126. https://doi.org/10.1111/j.1744-7402.2008.02187.x.

[52] A.J. Moulson, Reaction-bonded silicon nitride: its formation and properties, Journal of Materials Science 14 (1979) 1017–1051. https://doi.org/10.1007/BF00561287.
[53] J. Haggerty, A. Lightfoot, Opportunities for Enhancing the Thermal Conductivity of SiC and Si3N4 Ceramics Through Improved Processing, in: Ceramic Engineering and Science Proceedings, 2008: pp. 475–487. https://doi.org/10.1002/9780470314715.ch52.
[54] X. Zhu, Y. Zhou, K. Hirao, Effect of Sintering Additive Composition on the Processing and Thermal Conductivity of Sintered Reaction-Bonded Si_3N_4, Journal of the American Ceramic Society 87 (2004) 1398–1400. https://doi.org/10.1111/j.1151-2916.2004.tb07747.x.
[55] X. Zhu, Y. Zhou, K. Hirao, Z. Lenčéš, Processing and Thermal Conductivity of Sintered Reaction-Bonded Silicon Nitride. I: Effect of Si Powder Characteristics, Journal of the American Ceramic Society 89 (2006) 3331–3339. https://doi.org/10.1111/j.1551-2916.2006.01195.x.
[56] X. Zhu, Y. Zhou, K. Hirao, Z. Lenčéš, Processing and Thermal Conductivity of Sintered Reaction-Bonded Silicon Nitride: (II) Effects of Magnesium Compound and Yttria Additives, Journal of the American Ceramic Society 90 (2007) 1684–1692. https://doi.org/10.1111/j.1551-2916.2006.01462.x.
[57] K. Hirao, Y. Zhou, H. Hyuga, T. Ohji, D. Kusano, High Thermal Conductivity Silicon Nitride Ceramics, Journal of the Korean Ceramic Society 49 (2012) 380–384. https://doi.org/10.4191/kcers.2012.49.4.380.
[58] Y. Zhou, H. Hyuga, D. Kusano, Y. Yoshizawa, T. Ohji, K. Hirao, Development of high-thermal-conductivity silicon nitride ceramics, Journal of Asian Ceramic Societies 3 (2015) 221–229. https://doi.org/10.1016/j.jascer.2015.03.003.
[59] K. Hirao, K. Watari, H. Hayashi, M. Kitayama, High Thermal Conductivity Silicon Nitride Ceramic, MRS Bull. 26 (2001) 451–455. https://doi.org/10.1557/mrs2001.115.
[60] Y. Okamoto, N. Hirosaki, M. Ando, F. Munakata, Y. Akimune, Effect of sintering additive composition on the thermal conductivity of silicon nitride, J. Mater. Res. 13 (1998) 3473–3477. https://doi.org/10.1557/JMR.1998.0474.
[61] H. Yokota, M. Ibukiyama, Microstructure Tailoring for High Thermal Conductivity of β-Si3N4 Ceramics, Journal of the American Ceramic Society 86 (2003) 197–199. https://doi.org/10.1111/j.1151-2916.2003.tb03305.x.
[62] K. Sillapasa, S. Danchaivijit, K. Sujirote, Effects of Silicon Powder Size on the Processing of Reaction-Bonded Silicon Nitride, J Met Mater Miner 15 (2005).
[63] R. Nikonam-Mofrad, M.D. Pugh, R.A.L. Drew, A comparative study on nitridation mechanism and microstructural development of porous reaction bonded silicon nitride in the presence of CaO, MgO and Al_2O_3, Journal of Asian Ceramic Societies 8 (2020) 873–890. https://doi.org/10.1080/21870764.2020.1793471.
[64] X. Zhu, Y. Sakka, Textured silicon nitride: processing and anisotropic properties, Science and Technology of Advanced Materials 9 (2008) 033001. https://doi.org/10.1088/1468-6996/9/3/033001.
[65] N. Hirosaki, S. Ogata, C. Kocer, H. Kitagawa, Y. Nakamura, Molecular dynamics calculation of the ideal thermal conductivity of single-crystal α- and β − Si 3 N 4, Phys. Rev. B 65 (2002) 134110. https://doi.org/10.1103/PhysRevB.65.134110.
[66] B. Li, L. Pottier, J.P. Roger, D. Fournier, K. Watari, K. Hirao, Measuring the anisotropic thermal diffusivity of silicon nitride grains by thermoreflectance microscopy, Journal of the European Ceramic Society 19 (1999) 1631–1639. https://doi.org/10.1016/S0955-2219(98)00258-1.
[67] K. Hirao, K. Watari, M.E. Brito, M. Toriyama, S. Kanzaki, High Thermal Conductivity in Silicon Nitride with Anisotropie Microstructure, Journal of the American Ceramic Society 79 (1996) 2485–2488. https://doi.org/10.1111/j.1151-2916.1996.tb09002.x.

[68] K. Hirao, T. Nagaoka, M.E. Brito, S. Kanzaki, Microstructure Control of Silicon Nitride by Seeding with Rodlike β-Silicon Nitride Particles, Journal of the American Ceramic Society 77 (1994) 1857–1862. https://doi.org/10.1111/j.1151-2916.1994.tb07062.x.
[69] K. Hirao, M. Ohashi, M.E. Brito, S. Kanzaki, Processing Strategy for Producing Highly Anisotropic Silicon Nitride, Journal of the American Ceramic Society 78 (1995) 1687–1690. https://doi.org/10.1111/j.1151-2916.1995.tb08871.x.
[70] K. Watari, K. Hirao, M.E. Brito, M. Toriyama, S. Kanzaki, Hot Isostatic Pressing to Increase Thermal Conductivity of Si_3N_4 Ceramics, J. Mater. Res. 14 (1999) 1538–1541. https://doi.org/10.1557/JMR.1999.0206.
[71] Y. Akimune, F. Munakata, K. Matsuo, N. Hirosaki, Y. Okamoto, K. Misono, Raman Spectroscopic Analysis of Structural Defects in Hot Isostatically Pressed Silicon Nitride., Journal of the Ceramic Society of Japan 107 (1999) 339–342. https://doi.org/10.2109/jcersj.107.339.
[72] Y. Sakka, T.S. Suzuki, Textured Development of Feeble Magnetic Ceramics by Colloidal Processing Under High Magnetic Field, J. Ceram. Soc. Japan 113 (2005) 26–36. https://doi.org/10.2109/jcersj.113.26.
[73] Y. Sakka, T.S. Suzuki, T. Uchikoshi, Fabrication and some properties of textured alumina-related compounds by colloidal processing in high-magnetic field and sintering, Journal of the European Ceramic Society 28 (2008) 935–942. https://doi.org/10.1016/j.jeurceramsoc.2007.09.039.
[74] X.W. Zhu, Y. Sakka, T.S. Suzuki, T. Uchikoshi, S. Kikkawa, The c-axis texturing of seeded Si3N4 with β-Si3N4 whiskers by slip casting in a rotating magnetic field, Acta Materialia 58 (2010) 146–161. https://doi.org/10.1016/j.actamat.2009.08.064.
[75] C. Yang, J. Ding, J. Ma, B. Zhang, F. Ye, Y. Wu, Q. Liu, Microstructure tailoring of high thermal conductive silicon nitride through addition of nuclei with spark plasma sintering and post-sintering heat treatment, Journal of Alloys and Compounds 785 (2019) 89–95. https://doi.org/10.1016/j.jallcom.2018.12.204.

Submitted: 15.06.2024.

Revised: 21.08.2024.

Accepted: 23.08.2024.